

Aerodynamic roughness height for gravel-mantled megaripples, with implications for wind profiles near TARs on Mars



J.R. Zimelman ^{a,*}, S.P. Scheidt ^{a,b}, S.L. de Silva ^c, N.T. Bridges ^d, M.G. Spagnuolo ^{c,e}, E.M. Neely ^c

^aCEPS/NASM MRC 315, Smithsonian Institution, Washington, DC 20013-7012, United States

^bLunar and Planetary Laboratory, University of Arizona, 1629 E University Blvd, Tucson, AZ 85721, United States

^cCollege of Earth, Ocean, and Atmospheric Sciences, Oregon State University, Corvallis, OR 97331, United States

^dJohns Hopkins University Applied Physics Laboratory, Laurel, MD 20723, United States

^eIDEAN, UBA-CONICET, Ciudad de Bs. As., Argentina

ARTICLE INFO

Article history:

Received 15 May 2015

Revised 30 October 2015

Accepted 2 November 2015

Available online 14 November 2015

Keywords:

Earth

Geological processes

Mars, surface

ABSTRACT

Aerodynamic roughness heights of 1–3 cm were obtained from measured wind profiles collected among fields of gravel-mantled megaripples in the high desert of the Puna region of northwestern Argentina. Roughness height appears to be relatively insensitive to the angle at which the wind was incident upon the bedforms throughout the study sites. The results represent the first wind profiling measurements for large megaripples, but they also demonstrate the importance of a careful evaluation of many potential effects that can influence the utility of wind profiling data. The same effects that influence collection of fieldwork data must also be considered in any prediction of wind profiles anticipated to occur near Transverse Aeolian Ridges and other aeolian features on Mars that are intermediate in scale between wind ripples and small sand dunes.

Published by Elsevier Inc.

1. Introduction

Gravel-mantled megaripples, some with heights exceeding one meter, are present in portions of the Puna high desert region of northwestern Argentina (Milana, 2009; de Silva et al., 2013). The megaripple gravels consist of a bimodal association of dense ($>2 \text{ g cm}^{-3}$) low-albedo volcanic and metamorphic clasts up to 2.5 cm in diameter, along with high-albedo pumice clasts ($<1.5 \text{ g cm}^{-3}$) up to 5 cm in diameter, typically concentrated in a surface layer $<30 \text{ cm}$ in thickness, all overlying a fine-grained interior displaying local layering that is conformable to the underlying bedrock surface (de Silva et al., 2013). The Puna gravel-mantled megaripples were investigated in order to evaluate these features as analogs for Transverse Aeolian Ridges on Mars (de Silva et al., 2013; Bridges et al., 2015). One aspect of the overall project was to determine the aerodynamic roughness height (z_0) associated with these large aeolian bedforms, a parameter that is critical to understanding the work that can be done by the wind on a particulate surface exposed to an atmosphere. This report presents z_0 results derived from wind profile measurements collected at four sites within the Puna study area. The gravel-mantled megaripples in the Puna represent an important end member in the range of aeolian features that is included within the general term

‘megaripple’ (Greeley and Iversen, 1985). The Puna wind profile data were collected during two field trips that took place in December 2010 and November 2013.

The wind profiles provide the first estimate of z_0 for gravel-mantled megaripples throughout the Puna study area, but perhaps as significant, they also suggest that the largest gravel-mantled megaripples appear to induce flow separation, similar to what occurs near sand dunes (Walker and Nickling, 2002). The largest gravel-mantled megaripples seem to affect the wind profile more like a sand dune than like a typical sand ripple, which has implications for the roughness height expected near Transverse Aeolian Ridges (TARs) on Mars, a non-genetic term applied to large aeolian bedforms that are wide-spread across the planet that may have formed either as small sand dunes or large wind ripples (Bourke et al., 2003; Wilson and Zimelman, 2004; Balme et al., 2008; Berman et al., 2011). The Puna has also been proposed as an analog to investigate a possible genetic relationship between the gravel-mantled megaripples and ‘periodic bedrock ridges’, erosional bedforms with physical dimensions similar to the gravel-mantled megaripples; periodic bedrock ridges were first identified on Mars (Montgomery et al., 2012) but they have also been studied in the Puna (Hugenholtz et al., 2015). The differences of atmospheric density and gravity between Earth and Mars (Greeley and Iversen, 1985, pp. 82–85; Kok et al., 2012; Lorenz and Zimelman, 2014, pp. 40–48) do not diminish the importance of surface-wind

* Corresponding author.

(aeolian) interactions being strongly dependent upon z_0 for natural surfaces present on both planets.

2. Methodology

Wind profile data were collected at four sites within the Puna: Campo Piedra Pomez (CPP) [S26°34'59.0", W67°28'17.2", 3060 m elevation (WGS84)], White Barchan [S26°35'55.8", W67°26'39.9", 3030 m], Campo Purulla [S26°36'46.6", W67°46'03.6", 3380 m], and Salar de Incahuasi [S26°28'59.1", W67°41'03.8", 3310 m]. The regional setting for each of these study areas is described in detail in [de Silva et al. \(2013\)](#). Wind velocity profiles were measured using three SPER Scientific anemometers that record maximum, minimum and average wind speed (0.1 m/s accuracy, $\pm 2\%$ precision) during a time interval determined by the manual start and stop times of the recording period. We documented all three values for each anemometer after each run ([Table 1](#)), but it is important to note that only the average value captures all of the instantaneous readings throughout the sampling period. The maximum and minimum values indicate the magnitude of the fluctuations encountered during the sampling period, but there is no way to tell whether the maximum or minimum values occurred at the same instant at all three anemometers. Hence, it would not be reliable to derive z_0 using the maximum or minimum values; here we only use the average values for evaluating the characteristics of the wind profile. Due to occasional fluctuations in both wind strength and direction during the Puna trips, most wind profile data were collected during 2-min recording intervals. Studies of the averaging interval used for wind profile measurements indicate little loss of precision occurs when going from recording periods of 15 min to less than 1 min ([Namikas et al., 2003](#)), in agreement with recent tests that gave consistent results using our equipment for sampling periods ranging from 10 s to 7 min. Longer recording periods (up to several hours) and towers with more anemometers (>5) would certainly improve the accuracy of z_0 obtained from wind velocity profiles ([Bauer et al., 1992](#); [Wieringa, 1993](#); [Marticorena et al., 2006](#)), but the short time available at each site in the Puna led to the choice to collect multiple wind profiles at multiple locations at diverse sites rather than collect long time averages for a single tower location at one site (but see [Section 4](#)). Due to the length of time required to commute to and from the study sites, all wind measurements were obtained during the afternoon at times when the horizontal winds were strong so that inertial forces should dominate the wind flow, but we do not have the information needed to make a more detailed assessment of atmospheric stability (e.g., [Marticorena et al., 2006](#)) at each Puna site.

The three anemometers were logarithmically spaced with height above the surface, measured to the center of the spinning vane on each sampling head; anemometer readings and corresponding heights are listed in [Table 1](#). The three anemometers were affixed to a thin portable pole that was faced into the wind prior to each recording session ([Fig. 1](#)), mounted in a manner that did not interfere with wind flow to the sensor heads. A logarithmic least-squares fit (with correlation coefficient r^2) was applied to the wind profile data for each run, from which the height above the surface at which the wind velocity is zero (z_0) was determined. The fit used an expression of the form $y = a + b \ln x$, where y is the observed wind speed at height x above the surface. The fitting procedure worked well as long as the wind profile followed the normal logarithmic relationship present within a turbulent boundary layer generated through friction between the surface and the wind. The surface relief and particle sizes at each tower location were consistent for long fetches upwind from the tower; using Google Earth after the trips, the upwind fetch was consistent for >900 m at the CPP site, >160 m at the White Barchan

site, >400 m at the Purulla site, and >300 m at the Incahuasi site. These fetch lengths should be sufficient for development of a well-mixed boundary layer at the tower locations, as discussed by [Wieringa \(1993\)](#) and in [Section 4](#).

Setting $y = 0$, the best-fit expression is solved for x , which gives the value of z_0 ([Table 1](#)). When z_0 and the wind speed at one height are known, the wind speed at any other height is obtained using the Prandtl–von Karman logarithmic relationship known as the “Law of the Wall” ([Walker and Nickling, 2002](#); [Kok et al., 2012](#)): $u(z) = (u_* / k) \ln (z / z_0)$, where u is the wind velocity at height z , u_* is the shear velocity (or friction speed) of the wind, and k is the von Karman constant (normally taken to be 0.4). Using z_0 and the wind speed measured at each height, the Law of the Wall gives the shear velocity u_* (a measure of the slope of a semi-logarithmic profile of velocity versus height) of the wind for each anemometer reading. The rightmost column in [Table 1](#) lists the average of the three shear velocities calculated for the observed wind speeds measured by each anemometer during each recording session. In general, typical u_* values range from 0.2 m/s (for well sorted fine sand both in wind tunnels and in a field setting) to 0.4 m/s (field measurements in diverse desert settings) at the [threshold of sand motion](#) ([Bagnold, 1941](#); [Greeley and Iversen, 1985](#); [Nickling, 1988](#); [Lancaster and Baas, 1998](#); [Creysse et al., 2009](#); [Kok et al., 2012](#)). The elevation of the Puna means that the atmospheric pressure and density is considerably lower than at sea level, which translates to the shear velocity at the Puna being about $1.7\times$ the value at sea level; hence, threshold shear velocity at the Puna study sites should be more like 0.4–0.7 m/s ([de Silva et al., 2013](#); [Bridges et al., 2015](#)).

Topographic profiles of a gravel-mantled megaripple at each site were measured perpendicular to the bedform crest ([Fig. 2](#)). At the three 2010 sites the profile data were obtained by measuring the relief relative to a laser line projected above the megaripple bedform (following the procedure described in [Zimbelman et al. \(2012\)](#)). During the 2013 trip, a new profiling technique was used at the Incahuasi site. Through collection of many digital images taken along a line perpendicular to one gravel-mantled megaripple crest, multi-view stereo photogrammetry (MVSP) software was used to generate a digital terrain model (DTM) from which a detailed topographic profile across the feature was obtained ([Scheidt et al., 2014](#)). Local slope was removed from each topographic profile where the measurements clearly revealed breaks in slope on both sides of the bedform. The topographic profiles ([Fig. 2](#)) are representative of the gravel-mantled megaripples present at each wind profile location.

3. Results

The wind profile data from the CPP site were the first to be collected, and they are unique in that a strong afternoon wind was blowing from a direction almost parallel to the gravel-mantled megaripple crests (see [Supplemental Material Fig. S1](#)). This persistent strong wind direction was not typical of the formative winds responsible for the construction of the gravel-mantled megaripple bedforms, but the roughness height values of 1–3 cm obtained here are consistent with results obtained from the other Puna study locations ([Table 1](#)). The gravel-mantled megaripples at the CPP site are generally >80 cm in vertical relief ([Fig. 2](#)), with wavelengths >14 m, which represent the largest bedforms encountered at the four Puna wind profiling study sites. There is no significant change in z_0 obtained from wind tower locations distributed at various positions along a line perpendicular to the gravel-mantled megaripples at the CPP site, interpreted to suggest that the derived roughness height is a result of wind flow over a large portion of the megaripple field rather than being overly influenced by the nearest

Table 1
 Aerodynamic roughness height (z_0) and average shear velocity (u_*) derived from logarithmic least-squares regression (with correlation coefficient r^2) to wind profiles in the Puna of Argentina. Anemometer heights remain constant for subsequent entries until new heights are listed. Measurement sampling duration was 2 min except for one run at White Barchan. **Bold** entries indicate a non-logarithmic profile with height at the crest and downwind of a Purulla megaripple (see text).

| Site | Velocity (at height, in cm) | | | Roughness height z_0 (cm) | Corr. coeff. r^2 | Shear vel. u_* (m/s) |
|---|-----------------------------|-----------------|-----------------|--------------------------------|-----------------------|---------------------------|
| | v_1 (m/s) | v_2 (m/s) | v_3 (m/s) | | | |
| <i>Campo Piedra Pomez (CPP) (12/5/10)</i> | | | | | | |
| Trough ^a | Max | 7.3 (9) | 9.6 (39) | 18.4 (159) | 1.9 | 0.93 |
| | Ave | 6.3 | 7.9 | 15.9 | | |
| | Min | 4.6 | 5.5 | 11.1 | | |
| Trough ^a | Max | 6.9 | 9.6 | 18.4 | 1.7 | 0.93 |
| | Ave | 5.9 | 7.4 | 14.5 | | |
| | Min | 4.1 | 4.9 | 12.9 | | |
| Stoss base ^a | Max | 5.7 | 9.5 | 18.2 | 3.3 | 0.97 |
| | Ave | 4.9 | 8.5 | 16.6 | | |
| | Min | 2.9 | 5.8 | 12.4 | | |
| Stoss base ^a | Max | 4.3 | 8.1 | 16.2 | 3.7 | 0.98 |
| | Ave | 3.5 | 6.4 | 12.6 | | |
| | Min | 2.3 | 4.7 | 8.9 | | |
| Crest ^a | Max | 10.8 | 13.5 | 24.6 | 0.13 | 0.91 |
| | Ave | 9.3 | 11.5 | 23.4 | | |
| | Min | 6.6 | 8.0 | 16.5 | | |
| Crest ^a | Max | 12.0 | 14.6 | 24.7 | 0.60 | 0.94 |
| | Ave | 7.7 | 9.7 | 16.5 | | |
| | Min | 5.6 | 6.7 | 9.1 | | |
| Trough ^a | Max | 6.8 (8) | 10.1 (38) | 17.8 (158) | 0.94 | 0.99 |
| | Ave | 5.3 | 8.6 | 12.8 | | |
| | Min | 3.9 | 6.5 | 10.4 | | |
| Trough ^a | Max | 6.1 | 10.4 | 15.6 | 1.4 | 0.98 |
| | Ave | 5.2 | 8.3 | 13.7 | | |
| | Min | 3.3 | 5.1 | 8.8 | | |
| <i>White Barchan (12/5/10)</i> | | | | | | |
| Trough ^b | Max | 5.1 (8) | 7.9 (39) | 13.7 (160) | 2.1 | 0.96 |
| | Ave | 4.0 | 6.2 | 11.8 | | |
| | Min | 2.4 | 4.2 | 9.3 | | |
| Trough ^b | Max | 3.7 | 5.8 | 12.7 | 3.0 | 0.94 |
| | Ave | 2.9 | 4.4 | 9.8 | | |
| | Min | 2.1 | 3.3 | 7.6 | | |
| Trough ^b | Max ^d | 6.7 | 9.0 | 13.1 | 1.1 | 0.98 |
| | Ave ^d | 2.8 | 4.3 | 6.8 | | |
| | Min ^d | 1.7 | 2.7 | 5.0 | | |
| <i>Campo Purulla (12/6/10)</i> | | | | | | |
| Trough ^c | Max | 3.9 (11) | 6.9 (43) | 7.8 (162) | 3.0 | 0.99 |
| | Ave | 1.2 | 2.9 | 3.9 | | |
| | Min | 1.0 | 2.3 | 3.0 | | |
| Trough ^b | Max | 4.9 | 7.2 | 8.9 | 2.3 | 0.96 |
| | Ave | 3.1 | 4.3 | 7.8 | | |
| | Min | 1.3 | 2.9 | 4.5 | | |
| Trough ^b | Max | 3.9 | 6.3 | 8.1 | 2.0 | 0.98 |
| | Ave | 2.0 | 2.9 | 4.9 | | |
| | Min | 1.4 | 2.4 | 3.8 | | |
| Crest ^b | Max | 9.4 (11) | 9.9 (43) | 11.1 (161) | <1 E–10 | 0.96 |
| | Ave | 7.8 | 8.0 | 8.6 | | |
| | Min | 3.8 | 3.8 | 4.1 | | |
| Crest ^b | Max | 8.8 | 7.8 | 9.6 | <1 E–07 | 0.94 |
| | Ave | 5.9 | 6.1 | 7.0 | | |
| | Min | 3.8 | 5.2 | 4.3 | | |
| Crest ^b | Max | 14.0 | 10.3 | 12.8 | >200 | –0.65 |
| | Ave | 7.4 | 5.1 | 5.9 | | |
| | Min | 4.5 | 4.3 | 4.7 | | |
| Lee base ^b | Max | 4.7 | 4.3 | 7.4 | 1.0 | 0.86 |
| | Ave | 2.7 | 2.7 | 5.3 | | |
| | Min | 1.0 | 1.8 | 3.4 | | |
| Lee base ^b | Max | 3.6 | 3.1 | 5.8 | 9.5 | 0.98 |
| | Ave | 0.5 | 2.0 | 5.0 | | |
| | Min | 0.0 | 1.0 | 3.3 | | |
| Trough ^b | Max | 4.3 (12) | 4.3 (44) | 7.6 (162) | | |

Table 1 (continued)

| Site | | Velocity (at height, in cm) | | | Roughness height z_0 (cm) | Corr. coeff. r^2 | Shear vel. u_* (m/s) |
|--------------------------------------|---------------------|-----------------------------|-------------|-------------|--------------------------------|-----------------------|---------------------------|
| | | v_1 (m/s) | v_2 (m/s) | v_3 (m/s) | | | |
| | Ave | 2.6 | 2.5 | 4.6 | 0.60 | 0.84 | |
| | Min | 1.6 | 2.0 | 2.9 | | | |
| | Trough ^b | Max | 8.2 | 5.9 | | | 9.8 |
| | Ave | 5.5 | 4.3 | 7.4 | <0.01 | 0.61 | |
| | Min | 4.0 | 2.8 | 5.3 | | | |
| <i>Salar de Incahuasi (11/19/13)</i> | | | | | | | |
| Trough ^b | Max | 4.7 (10) | 6.7 (40) | 10.7 (160) | 1.2 | 0.93 | 0.6 |
| | Ave | 3.7 | 4.4 | 7.9 | | | |
| | Min | 1.7 | 2.1 | 3.6 | | | |
| Trough ^b | Max | 8.4 | 9.9 | 14.9 | 0.49 | 0.93 | 0.6 |
| | Ave | 5.3 | 6.0 | 9.7 | | | |
| | Min | 1.2 | 2.3 | 3.0 | | | |
| Trough ^b | Max | 6.4 | 9.8 | 14.6 | 0.55 | 0.99 | 0.6 |
| | Ave | 4.5 | 6.3 | 8.7 | | | |
| | Min | 0.0 ^e | 3.2 | 4.8 | | | |

^a Wind was blowing 15° from parallel to the crest.

^b Wind was blowing perpendicular to the crest.

^c Wind was blowing 20° from parallel to the crest.

^d 22 min sampling duration.

^e This value is questionable; the overall wind seemed relatively constant throughout the sampling period to an observer positioned behind the tower.



Fig. 1. Wind profile equipment in a trough between megaripples at the Purulla site, looking north. Subsequent measurements were obtained at locations across the megaripple to the right of the tower. JRZ photo, 12/6/10.

bedform. However, smaller z_0 values were obtained at the CPP site when the tower was placed on the crest of a megaripple (Table 1), which also correspond to the strongest wind speeds observed at any of the Puna tower sites. The height of the CPP megaripple

bedforms (Fig. 2) placed the crest tower location well above the height of the other CPP tower sites, which may possibly have contributed to a higher overall wind speed at this location. All wind speeds at the CCP site were above threshold shear velocity, but

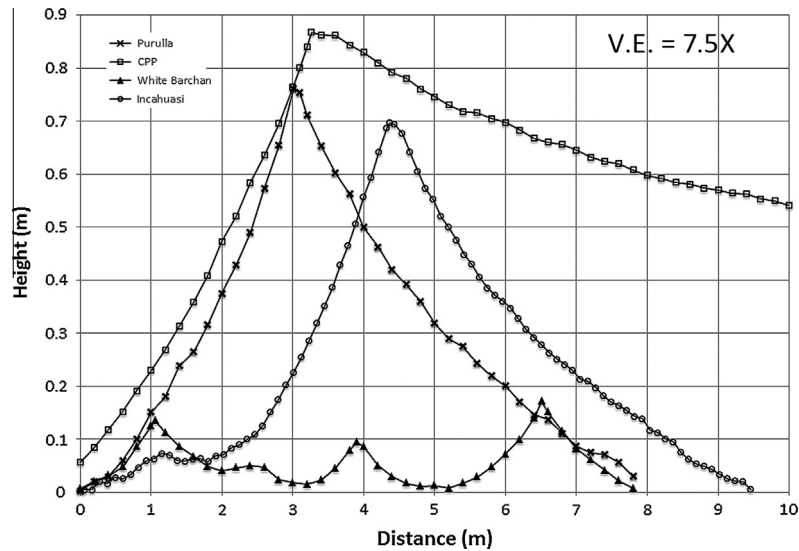


Fig. 2. Combined plot of megaripple profiles measured perpendicular to the megaripple crests. Profiles are shown at the same scale, oriented so that the formative wind comes from the left for each site. The precision of the measurement for each point is smaller than the symbols shown in the plot. See text for the methods used to produce these profiles.

only occasional saltating sand grains were observed during the wind profile measurements, indicating a lack of a substantial upwind sand supply at the time of the measurements.

At the White Barchan site, the wind was blowing perpendicular to the megaripple crests during the profile measurements (SM Fig. S2). The White Barchan megaripples are best described as granule-covered features, given the 2–3 mm size of the milky quartz coarse particles on their surface (SM Fig. S7), in contrast to the gravel mantling on the large bedforms at the other Puna study sites (megaripple crest particles at each site are shown in SM Figs. S5 and S7–S9). The White Barchan granule ripples are the smallest bedforms at the four Puna study sites (Fig. 2), with vertical relief of 10–20 cm, which is comparable to granule ripples in diverse desert locations (Sharp, 1963; Yizhaq et al., 2009; Zimelman et al., 2012). In spite of the small bedform and surface particle size at this location, our experimental setup was not capable of distinguishing effects attributable to these smaller physical dimensions; a roughness height of 1–3 cm was obtained here as well (Table 1). The lowest measured z_0 values at the White Barchan site come from of a 22-min-long observation session, the only Puna measurements obtained for a sampling period longer than 2 min.

The Purulla site was the first location where wind profile data were obtained with wind blowing both along and perpendicular to the crest orientation of large gravel-mantled megaripples. The Purulla megaripples have 75 cm of vertical relief (Fig. 2) and wavelength >11 m. During the first Purulla wind profiling measurement, the wind blew almost parallel to the megaripple crests, similar to the situation encountered during profiling at the CCP site; a z_0 of 3 cm was obtained from this profiling run, at a shear velocity only slightly above threshold (Table 1). Following the first profiling measurement, the wind underwent a pronounced shift to an orientation perpendicular to the bedform crests. The anemometer pole was rotated (while at the same location) to face the anemometers into the new wind orientation, after which two profiling runs yielded z_0 of 2.0–2.3 cm for shear velocities comparable to those during the first measurement (Table 1). The fact that the results obtained at this tower location, in the trough between two megaripples (Fig. 1), are consistent for two rather different wind orientations, as well as with the overall CCP results, suggest an insensitivity to a specific wind orientation, although more precise measurements may be needed in order to distinguish any subtle orientation-dependent changes.

Subsequent Purulla profiling locations placed the tower at positions on (Fig. 3) and downwind of (SM Fig. S3) a large gravel-mantled megaripple. At these locations, the wind profiles were non-logarithmic; the lowest anemometer speeds were comparable to or even higher than the speeds at the second anemometer, resulting in spurious z_0 values when applied to a logarithmic fit (Table 1). At the time, we suspected that perhaps the lower anemometer may have malfunctioned, and this assessment ended the wind profiling measurements for the 2010 trip. However, once back home, all three anemometers were found to be functioning properly, giving consistent wind results to within 0.1 m/s when placed adjacent to each other in a constant wind, leading to the conclusion that accurate speeds had been recorded at Purulla.

Following the first trip, an extensive literature search revealed multiple investigations of non-logarithmic wind profiles associated with wind flow over sand dunes (e.g., Fraser et al., 1998; Hesp, 2002; Walker and Nickling, 2002). Much of the non-logarithmic behavior over dunes can be attributed to the speed-up of near-surface winds caused by flow compression on the stoss side (e.g., the Bernoulli principle in action; Walker and Nickling, 2002), along with formation of a separation bubble downwind of the dune crest (e.g., Sauer mann et al., 2001; Kroy et al., 2002; Duran et al., 2010; Walker and Shugar, 2013). The Purulla wind profiling results from locations on and immediately downwind of a large megaripple suggest that flow separation may take place at the gravel-mantled megaripple crest, along with development of a turbulent wake zone downwind, something we had not anticipated. Unfortunately, the anemometers do not record wind direction, so we are unable to confirm that reverse flow actually took place at Purulla.

During the 2013 trip, we intended to investigate the possibility of flow separation downwind of large megaripples, but due to multiple cable failures early in the profiling effort, useful wind profiling measurements were obtained for only a single tower location at the Incahuasi site. The gravel-mantled megaripples at the Incahuasi site have vertical relief and wavelength very similar to that of the Purulla site (Fig. 2). The Incahuasi tower site was chosen to be >5 m downwind from the nearest upwind gravel-mantled megaripple, in order to be well beyond the likely end of any separation bubble (SM Fig. S4). Wind profiles obtained from three 2-min sampling periods at this location gave good logarithmic wind profiles and z_0 of 0.5–1.2 cm for wind perpendicular to the gravel-mantled megaripple crests, at shear velocities above what should



Fig. 3. Tower on crest of a megaripple at the Purulla site. Wind was blowing perpendicular to the megaripple crest. A non-logarithmic wind profile was observed at this location, possibly related to the Bernoulli effect of compressed flow lines moving up the stoss side of the bedform. JRZ photo, 12/6/10.

be the local threshold for sand saltation (Table 1). As at all other Puna megaripples sites, virtually no sand was observed to be in motion at the Incahuasi site, likely due to limited upwind sand supply. The minimum wind speed for the lowest anemometer gave a null result at the conclusion of the third measurement period, followed quickly by complete failure of the middle anemometer; both anemometers failed to produce any useful results after this third measurement period, most likely due to failures in the cables leading from the anemometers to the recording meters. After several aborted attempts to find a way to resolve this issue in the field, we abandoned further wind profile measurements during the 2013 trip. Upon returning from the 2013 trip, we concluded that it would not be productive to replace the failed anemometers, for reasons discussed in the next section.

4. Discussion

After the completion of both Puna trips, the review process brought to our attention a very important paper that would have greatly assisted both the preparation for and the performance of wind profiling experiments in the field. Wieringa (1993) made an in-depth assessment of several conditions that can affect the usefulness of wind profiling measurements aimed at determining roughness height, published in a journal that is likely unfamiliar to most geologists. This paper includes both an excellent review of the theory of wind flow within a boundary layer, the region between steady stream flow and a solid (or mobile) surface boundary, and explanations of several conditions that govern the collection of meaningful wind profile measurements; this paper should be required reading for everyone contemplating making wind

profile measurements in a field (or laboratory) setting. We only became aware of this paper after the Puna data had already been collected, but next we consider how the Puna measurements compare to the guidelines of Wieringa (1993).

The region of interaction between the wind and the surface can be described by several terms, but the concept of the ‘inertial sub-layer’ (ISL; Wieringa, 1993) has an effect on how and where wind profile measurements should be made. In particular, the lower limit to the ISL, below which the wind flow transitions from true turbulent flow to more laminar flow, should be at least $20z_0$ (Wieringa, 1993). Consequently, an estimate of z_0 is needed before the lowest anemometer height can be determined. The Puna z_0 values obtained here suggest that the lowest anemometer should have been at a height of at least 20 cm above the surface, so it is quite probable that our lowest anemometer was located below the bottom of a ‘well-mixed’ ISL, but there is no indication that the lowest anemometer results from the Puna were somehow consistently skewed or modified, except immediately downwind of large megaripples. The upper limit to the ISL is related to the planetary (global-scale) boundary layer at the study location, and our small tower was much shorter than what could be expected for the scale of the planetary boundary layer at the Puna.

Measuring a wind profile can also be affected by the upwind fetch, the length over which the surface has a homogeneous distribution of roughness elements. Once again, the minimum fetch length for development of a well-mixed ISL is related to the roughness height of the surface, so an estimate of z_0 should normally precede selection of a tower location. For roughness heights on the order of 10 cm, the minimum fetch should be about 100 times the lowest anemometer height (Fig. 3 of Wieringa (1993)), which

from above should be $20z_0$. Consequently, for the Puna study sites, the minimum fetch lengths should have been >200 m. Google Earth allowed us to determine the upwind fetch length at each tower site (described above), with the result that the Puna tower locations exceeded or were close to the recommended minimum upwind fetch length.

The number of levels at which the wind speed should be measured is also a function of the surface roughness of the study site. In order to determine z_0 to within a factor of 2, 4 levels should be documented for $z_0 \sim 0.1$ m, with 5 or more levels needed for really smooth terrains (Wieringa, 1993). Since the Puna tower used three anemometers for all of the measurements, the resulting z_0 values in Table 1 could be uncertain by more than a factor of two. However, the 3-anemometer setup used at the Puna typically obtained results consistent with the Law of the Wall, except immediately downwind of large megaripples, and it was successful obtaining reasonable z_0 values at some other desert settings (discussed below).

Wieringa (1993) mentioned that the equations used to describe wind flow within the ISL refer to a ‘neutral thermal stratification’ condition in the atmosphere. Marticorena et al. (2006) explored the thermal conditions associated with wind tower measurements in great depth, relating z_0 to several temperature profile conditions. We do not have temperatures for each anemometer height for the Puna measurements to address the stability question quantitatively, but the observed horizontal afternoon winds experienced while making the wind measurements suggest that inertial forces likely dominated over local convective instability.

The anemometers used in the Puna study recorded maximum, minimum and average wind speeds during each recording interval. As described in Section 2, there is no way to confirm that the maximum and minimum winds occurred at the same instant during the recording interval, and therefore both extreme values are not

useful for a quantitative assessment of the wind profile. For completeness all recorded values are reported in Table 1, but only the average values were used to determine z_0 and u_* . For future wind profiling experiments, we recommend that anemometers with a data logging capability (along with simultaneous temperature measurements) be employed, which would allow the wind strength variability to be assessed through the entire recording interval, as well as assess the atmospheric stability during the measurement interval. These considerations governed our choice not to replace the anemometers used for the Puna study with similar instruments.

The experimental set-up used in the Puna clearly has several limitations, as discussed above. In order to characterize the effects that these limitations may have had on the results, we compared results obtained with our equipment at other locations to values in the literature obtained over similar terrains using a more sophisticated apparatus. Table 2 gives z_0 results obtained with the same 3-anemometer tower used in the Puna to compare to well-constrained results reported in the literature from diverse settings. The z_0 range reported by Marticorena et al. (2006) also incorporates consideration of thermal stability conditions. These data demonstrate that the tower setup used in the Puna does reproduce small z_0 values for obstacle-free sand that are consistent with several previously published well documented studies. The sand sheet results obtained at the Killpecker dunes slightly exceed the range reported by Marticorena et al. (2006), but it is not clear how comparable in detail these two locations may be. The equipment used in the Puna also obtained values for grass-covered sand that are consistent with other published results. These comparisons do not account for all of the issues raised by Wieringa (1993) and Marticorena et al. (2006), but at least they suggest that the Puna results can be considered to be a first-order representation of what might be expected for wind flow within fields of megaripples.

Table 2
Comparison of roughness heights reported in the literature to those obtained at desert locations with the same 3-anemometer equipment used in this study. If only a single value was published, that value is listed in both the minimum and maximum columns. **Bold** entries are 3-anemometer measurements obtained on the specified date. Literature data are mostly derived from Tables 6 and 7 of Marticorena et al. (2006) and Table VIII of Wieringa (1993).

| Surface type | Ref. | Location | z_0 min (m) | z_0 max (m) |
|--|------|-----------------------|---------------|---------------|
| <i>Flat sand</i> | | | | |
| Bare sand sheet | [1] | Owens Lake, CA | .00075 | .00075 |
| Flat desert | [2] | Central Sahara | .0003 | .0003 |
| Flat sand, scattered rocks | [3] | McMurdo, Antarc. | .0005 | .0009 |
| Flat desert, tidal flat | [4] | Multiple sites | .0002 | .0005 |
| Interdunal surface | [5] | Gobabeb, Namibia | .00004 | .00004 |
| Sand dunes | [6] | Douz, Tunisia (S8) | .000019 | .00034 |
| Flat sand sheet^a | | Kau Desert, HI | .00002 | .00005 |
| Non-vegetated interdune^b | | Killpecker, WY | .00009 | .0006 |
| <i>Vegetated sand</i> | | | | |
| Sand sheet with salt grass | [1] | Owens Lake, CA | .002 | .013 |
| Short grass and moss | [4] | Multiple sites | .008 | .03 |
| Tundra | [7] | Peard Bay, AK | .021 | .021 |
| Vegetated surfaces | [6] | Tunisia (S2–5, 7, 10) | .0017 | .020 |
| Grass-covered sand sheet^c | | Killpecker, WY | .01 | .035 |
| <i>For comparison to Puna</i> | | | | |
| Gravelly sand sheets to boulder-covered moraines | [3] | McMurdo, Antarc. | .001 | .03 |
| Short grass and moss | [4] | Multiple sites | .008 | .03 |
| Vegetated, stony pasture | [6] | Tunisia (S3, S5) | .0046 | .015 |
| Gravel-covered megaripples | | This work | .01 | .03 |

[1] Lancaster and Baas (1998).

[2] Tezlaff (1974).

[3] Lancaster (2004).

[4] Wieringa (1993), from Table VIII – homogeneous surface types.

[5] Greeley et al. (1997).

[6] Marticorena et al. (2006).

[7] Harper and Wiseman (1977, 1978).

^a Data collected on 8/16/09.

^b Data collected on 7/12/06.

^c Data collected on 7/14/06.

Table 2 also shows that the Puna results are broadly similar to results obtained from gravel- to boulder-covered glacial terrain, as well as sites with short grass or in a vegetated, stony pasture. It appears that the gravel-mantled megaripple bedforms in the Puna influence the wind in a manner equivalent to that of a stony field or terrain covered by low plants. We interpret these comparisons to suggest that the Puna z_0 values are more likely a representation of wind flow over a broad region of megaripples rather than being dominated by a single nearby bedform (unless the measurements are made too close to an upwind large megaripple), or by the distribution of particles that coat the megaripple surfaces. If this is correct, then the Puna results represent a regional property more than a result that is somehow tied to an individual megaripple bedform.

The Puna study sites appear to have similar z_0 values regardless of the orientation of the wind relative to the crests of the bedforms (within the acknowledged limitations of the measurements). Unlike what we expected before the fieldwork, the Puna results hint that roughness height may not be closely tied to the orientation that the wind blows across a megaripple field. This possible orientation insensitivity also may be related to the observation that the crests of the large gravel-mantled megaripples consist of closely packed gravel particles (SM Figs. S5, S8, S9), while the troughs between large megaripples (SM Fig. S6) consist of more separated gravel particles, more comparable to the spacing of particles on the granule-coated White Barchan megaripples (SM Fig. S7). Somehow the combination of both the surface particle distribution and the scale of the large megaripples may contribute to an effective roughness height that does not demonstrate a strong directional dependence, although clearly more precise wind profile measurements are required to evaluate this possibility.

The Puna results have some broad implications for the possible aerodynamic roughness height associated with coarse-particle-mantled TARs on Mars. It is probable that the thin martian atmosphere would alter some of the limitations for wind profiling described by Wieringa (1993), such as the minimum and maximum heights at which to assess the ISL. Even without a detailed understanding of boundary layer details for Mars, the Wieringa (1993) guidelines should be considered when attempting to predict what wind profile may be associated with a TAR field. Some specific values recommended by Wieringa (1993) may turn out to be minimums for a planet where reduced atmospheric pressure and gravity (compared to Earth) both contribute to saltation paths that are substantially longer than those experienced on Earth (e.g., White, 1979).

Martian TARs are mantled by particles that are considerably larger than medium sand, as has been observed by rovers at multiple locations on Mars (e.g., Sullivan et al., 2005, 2008; Blake et al., 2013). Perhaps the difference between wind flow over a flat surface versus wind flow over a TAR field may contribute to both the initiation and growth of coarse-particle-mantled aeolian bedforms on Mars. The roughness height associated with a TAR field should affect how saltation, reptation, and creep processes express themselves with regard to the resulting bedforms. The Puna results should be viewed as warranting further careful investigation, both on Earth and for eventual application to Mars. Wind tunnel investigations of z_0 associated with scaled megaripple bedforms could be a productive area for future investigation, and also aid in preparations for future wind profiling experiments around megaripples on Earth or Mars.

Acknowledgments

This work was supported through a now-concluded NASA Mars Fundamental Research Program grant (NNX10AP79G) to Oregon State University (S.L. de Silva, P.I.), and analysis supplemented by

NASA Mars Data Analysis Program grant NNX12AJ38G (J.R. Zimbelman, P.I.). The patience of the Editor and the comments of two anonymous reviewers were very helpful in improving the manuscript, particularly one reviewer who patiently worked with us through multiple iterations and brought to our attention the important Wieringa (1993) and Marticorena et al. (2006) papers.

Appendix A. Supplementary material

Supplementary data associated with this article can be found, in the online version, at <http://dx.doi.org/10.1016/j.icarus.2015.11.008>.

References

- Bagnold, R.A., 1941. *The Physics of Blown Sand and Desert Dunes*. Chapman and Hall, London, p. 256p.
- Balme, M. et al., 2008. Transverse aeolian ridges (TARs) on Mars. *Geomorphology* 101, 703–720. <http://dx.doi.org/10.1016/j.geomorph.2008.03.011>.
- Bauer, B.O., Sherman, D.J., Wolcott, J.F., 1992. Sources of uncertainty in shear stress and roughness length estimates derived from velocity profiles. *Prof. Geogr.* 44 (4), 453–464. <http://dx.doi.org/10.1111/j.0033-0124.1992.00453.x>.
- Berman, D.A. et al., 2011. Transverse Aeolian Ridges (TARs) on Mars II: Distributions, orientations, and ages. *Icarus* 213, 116–130. <http://dx.doi.org/10.1016/j.icarus.2011.02.014>.
- Blake, D.F. et al., 2013. Curiosity at Gale Crater, Mars: Characterization and analysis of the Rocknest sand shadow. *Science* 341. <http://dx.doi.org/10.1126/science.1239505>.
- Bourke, M.C., Wilson, S.A., Zimbelman, J.R., 2003. The variability of transverse aeolian ridges in troughs on Mars. *Lunar Planet. Sci.* XXXIV, Abstract 2090.
- Bridges, N.T. et al., 2015. Formation of gravel-mantled megaripples on Earth and Mars: Insights from the Argentinean Puna and wind tunnel experiments. *Aeol. Res.* 17, 49–60. <http://dx.doi.org/10.1016/j.aeolia.2015.01.007>.
- Creysseels, M. et al., 2009. Saltating particles in a turbulent boundary layer: Experiment and theory. *J. Fluid Mech.* 625, 47–74. <http://dx.doi.org/10.1017/S0022112008005491>.
- de Silva, S.L. et al., 2013. Gravel-mantled megaripples of the Argentinean Puna: A model for their origin and growth with implications for Mars. *Geol. Soc. Am. Bull.* 125 (11/12), 1912–1929. <http://dx.doi.org/10.1130/B30916.1>.
- Duran, O., Parteli, E.J.R., Hermann, H.J., 2010. A continuous model for sand dunes: Review, new developments and application to barchans dunes and barchan dune fields. *Earth Surf. Proc. Landforms* 35, 1591–1600. <http://dx.doi.org/10.1002/esp.2070>.
- Fraser, G.S. et al., 1998. Windflow circulation patterns in a coastal dune blowout, south coast of Lake Michigan. *J. Coastal Res.* 14 (2), 451–460.
- Greeley, R., Iversen, J.D., 1985. *Wind as a Geological Process on Earth, Mars, Venus, and Titan*. Cambridge Univ. Pr., New York, 333 p.
- Greeley, R. et al., 1997. Applications of spaceborne radar laboratory data to the study of aeolian processes. *J. Geophys. Res.* 102, 10971–10983.
- Harper, J.R., Wiseman, W.J., 1977. Temporal variation of surface roughness over a tundra surface. *J. Geophys. Res.* 82, 3495–3497.
- Harper, J.R., Wiseman, W.J., 1978. Correction to “Temporal variation of surface roughness over a tundra surface”. *J. Geophys. Res.* 83, 968.
- Hesp, P., 2002. Foredunes and blowouts: Initiation, geomorphology and dynamics. *Geomorphology* 48, 245–268.
- Hugenholtz, C.H., Barchyn, T.E., Favaro, E.A., 2015. Formation of periodic bedrock ridges on Earth. *Aeolian Res.* 18, 135–144. <http://dx.doi.org/10.1016/j.aeolia.2015.07.002>.
- Kok, J.F. et al., 2012. The physics of wind-blown sand and dust. *Rep. Prog. Phys.* 75, 106901. <http://dx.doi.org/10.1088/0034-4885/75/10/106901>.
- Kroy, K., Sauerbmann, G., Herrmann, H.J., 2002. Minimal model for sand dunes. *Phys. Rev. Lett.* 88, 054301. <http://dx.doi.org/10.1103/PhysRevLett.88.054301>.
- Lancaster, N., 2004. Relation between aerodynamic and surface roughness in hyper-arid old desert: McMurdo dry valleys, Antarctica. *Earth Surf. Proc. Landforms* 29, 853–867.
- Lancaster, N., Baas, A., 1998. Influence of vegetation cover on sand transport by wind: Field studies at Owens Lake, California. *Earth Surf. Proc. Landforms* 23, 69–82.
- Lorenz, R.D., Zimbelman, J.R., 2014. *Dune Worlds: How Windblown Sand Shapes Planetary Landscapes*. Springer/Praxis, Berlin, p. 308p.
- Marticorena, B. et al., 2006. Surface and aerodynamic roughness in arid and semiarid areas and their relation to radar backscatter coefficient. *J. Geophys. Res.* 111, F3017. <http://dx.doi.org/10.1029/2006JF000462>.
- Milana, J.P., 2009. Largest wind ripples on Earth? *Geology* 37, 343–346. <http://dx.doi.org/10.1130/G25382A.1>.
- Montgomery, D.R., Bandfield, J.L., Becker, S.K., 2012. Periodic bedrock ridges on Mars. *J. Geophys. Res.* 117, E03005. <http://dx.doi.org/10.1029/2011JE003970>.
- Namikas, S.L., Bauer, B.O., Sherman, D.J., 2003. Influence of averaging interval on shear velocity estimates for aeolian transport modeling. *Geomorphology* 53, 235–246. [http://dx.doi.org/10.1016/S0169-555X\(02\)00314-8](http://dx.doi.org/10.1016/S0169-555X(02)00314-8).

- Nickling, W.G., 1988. The initiation of particle movement by wind. *Sedimentology* 35, 499–511.
- Sauermaun, G., Kroy, K., Hermann, H.J., 2001. A continuum saltation model for sand dunes. *Phys. Rev. E* 64, 031305. <http://dx.doi.org/10.1103/PhysRevE.64.031305>.
- Scheidt, S.P., Zimbelman, J.R., Johnson, M.B., 2014. Multiview stereo photogrammetry of Mars aeolian analogs. *Lunar Planet. Sci. XLV*. Abstract 1446.
- Sharp, R.P., 1963. Wind ripples. *J. Geol.* 71, 617–636.
- Sullivan, R. et al., 2005. Aeolian processes at the Mars Exploration Rover Meridiani Planum landing site. *Nature* 436, 58–61. <http://dx.doi.org/10.1038/nature03641>.
- Sullivan, R. et al., 2008. Wind-driven particle mobility on Mars: Insights from Mars Exploration Rover observations at “El Dorado” and surroundings at Gusev Crater. *J. Geophys. Res. Planets* 113, E06S07. <http://dx.doi.org/10.1029/2008JE003101>.
- Tezlauff, G., 1974. Der warmehaushalt in der zentralen Sahara. *Ber. Inst. Meteorol. Klimatol., Univ. Hanover*, 13, 113 p.
- Walker, I.J., Nickling, W.G., 2002. Dynamics of secondary airflow and sediment transport over and in the lee of transverse dunes. *Prog. Phys. Geogr.* 26 (1), 47–75. <http://dx.doi.org/10.1191/0309133309pp325ra>.
- Walker, I.J., Shugar, D.H., 2013. Secondary flow deflection in the lee of transverse dunes with implications for dune morphodynamics and migration. *ESPL* 38 (14), 1642–1654.
- White, B.R., 1979. Soil transport by winds on Mars. *J. Geophys. Res.* 84, 4643–4651.
- Wieringa, J., 1993. Representative roughness parameters for homogeneous terrain. *Bound. Layer Meteorol.* 63, 323–363.
- Wilson, S.A., Zimbelman, J.R., 2004. The latitude-dependent nature and physical characteristics of transverse aeolian ridges on Mars. *J. Geophys. Res.* 109, E10003. <http://dx.doi.org/10.1029/2004JE002247>.
- Yizhaq, H. et al., 2009. Morphology and dynamics of aeolian megaripples in Nahal Kasey, Southern Israel. *Isr. J. Earth Sci.* 57, 149–165.
- Zimbelman, J.R., Williams, S.H., Johnston, A.K., 2012. Cross-sectional profiles of sand ripples, megaripples, and dunes: A method for discriminating between formational mechanisms. *Earth Surf. Proc. Landforms* 37, 1120–1125. <http://dx.doi.org/10.1002/esp.3243>.